

A Trinuclear Defect-Grid Iron(II) Spin Crossover Complex with a Large Hysteresis Loop that is Readily Silenced by Solvent Vapor**

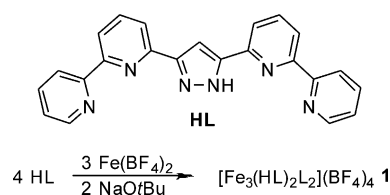
Markus Steinert, Benjamin Schneider, Sebastian Dechert, Serhiy Demeshko, and Franc Meyer*

Abstract: A new type of $[2 \times 2]$ matrix-like complexes with one vertex devoid of a metal ion has been selectively synthesized. The defect-grid triiron(II) complex exhibits a sharp and complete spin-crossover (SCO) from the 1HS-2LS to the 2HS-1LS state (HS: high spin; LS: low spin) with wide hysteresis near room temperature. Although the “structurally soft” H-bonded vertex, elastically coupled to the metal ions, accounts for the stabilization of spin states, it also mediates a dramatic, yet reversible, response to the uptake of exogenous solvent molecules leading to silencing of the SCO. The high sensitivity towards those guest molecules, the short response time upon exposure, and the smooth reversibility of guest binding are favorable characteristics for future sensing applications of such defect grids.

Spin-crossover (SCO) complexes undergo a spin switching induced by external stimuli such as changes of pressure or temperature, or by irradiation with light.^[1] Of particular interest are SCO systems that exhibit bistability in the form of an abrupt SCO transition with wide hysteresis, preferably around room temperature, because of their potential applications as materials for data storage or electronic display devices. It has been assumed that linking SCO units via bridging ligands should significantly enhance cooperativity and may lead to pronounced bistable behavior, which has motivated extensive research towards the development of bi- and oligonuclear SCO Fe^{II} complexes.^[2] Still, most of the reported complexes with hysteretic SCO are mononuclear or polymeric Fe^{II} compounds,^[3,4] while examples of dinuclear systems have been increasingly recognized only in recent years.^[5,6] Tri-^[7] and tetranuclear^[8–10] Fe^{II} SCO compounds are generally rather rare, with mostly gradual and incomplete SCO, and very few of them exhibit thermal hysteresis.^[11] Among the oligonuclear Fe^{II} complexes, squarelike $[2 \times 2]$ grid complexes currently receive particular attention because of their matrix-like arrangement of four addressable sites. This is potentially beneficial for data storage devices or quantum cellular automata, provided that the grids feature

certain switchability with respect to redox and/or spin states.^[10,12,13] Another sought-after feature of SCO complexes is the spin-state modulation through host–guest chemistry, where effects of the guest molecules are mediated by van der Waals interactions, hydrogen bonds, π – π interactions, or structural changes. Dynamic host–guest chemistry of that type has mostly been observed for porous 2D or 3D SCO materials, which makes them interesting candidates for potential sensing applications.^[14] In several studies, small solvent guest molecules have been found to induce^[15] or change^[4a,16] the SCO properties of the host, but there are also occasional reports where exposure to guest solvents inhibits a spin transition.^[6]

In previous work, we reported a robust and switchable $[2 \times 2]$ Fe₄ grid complex^[9] based on the pyrazole-bridged compartmental ligand HL (Scheme 1);^[17] the $[L_4Fe_4]^{4+}$ core featured multistability with respect to spin and redox states,



Scheme 1. Ligand HL and complex formation.

albeit without any hysteresis in the SCO transitions of the all-ferrous system. Slight modification of the HL ligand backbone then gave a $[2 \times 2]$ Fe₄ grid complex whose [HS-LS-HS-LS] mixed-spin state persisted over a wide temperature range, which is a favourable situation for use in quantum cellular automata.^[10] Furthermore, expansion of the grid core yielded a rhombic-like $[L_4Fe_2(Ag_2)_2]^{6+}$ complex with Ag₂ dumbbells at two opposite vertices.^[18] Herein we introduce the first example of an unprecedented class of matrix-like complexes derived from a $[2 \times 2]$ grid structure in which one of the vertices is devoid of a metal ion; we term it a defect-grid structure. As will be shown below, the trinuclear Fe^{II} complex $[Fe_3(HL)_2L_2](BF_4)_4$ (**1**) shows abrupt SCO, with the widest hysteresis loop reported to date for di- and oligonuclear molecular complexes.^[5g] Moreover, the SCO properties of **1** are guest-dependent and respond readily to exposure to a variety of solvent vapors.

Compound **1** was first discovered accidentally as a minor side product when the protocol for the synthesis of $[L_4Fe_4](BF_4)_4$ was varied. Subsequent optimization of the reaction conditions then revealed that **1** can be obtained in a targeted one-pot synthesis and in very good yields. Key to the selective

[*] Dipl.-Chem. M. Steinert, Dr. B. Schneider, Dr. S. Dechert, Dr. S. Demeshko, Prof. Dr. F. Meyer
Institut für Anorganische Chemie
Georg-August-Universität Göttingen
Tammannstrasse 4, 37077 Göttingen (Germany)
E-mail: franc.meyer@chemie.uni-goettingen.de
Homepage: <http://www.meyer.chemie.uni-goettingen.de>

[**] Financial support from the DFG (SFB 1073, project B06) is gratefully acknowledged.

Supporting information for this article is available on the WWW under <http://dx.doi.org/10.1002/ange.201403068>.

formation of the Fe_3 defect grid is the stoichiometry of the reaction, since the ligand HL, $\text{Fe}(\text{BF}_4)_2 \cdot 6\text{H}_2\text{O}$ and NaOtBu have to be combined in the proper ratios 4:3:2 (Scheme 1). Under these conditions half of the amount of ligand HL remains protonated, and one of the grid's corners lacks a metal ion but hosts the two NH protons that form two interligand hydrogen bonds (see below). Formation of the defect-grid product via the previously reported^[18] "corner" complex $[\text{Fe}(\text{HL})_2]^{2+}$ ^[10] can be conveniently monitored by UV/Vis spectroscopy and ESI mass spectrometry (Figures S2 and S3 in the Supporting Information). A dominant ESI-MS peak for the tetracation $[\text{Fe}_3(\text{HL})_2\text{L}_2]^{4+}$, with the expected isotopic distribution pattern, reflects the integrity of the defect-grid structure in MeCN solution and suggests its high stability and its inertness even in the presence of potentially coordinating solvents.

Single crystals of **1**·MeCN could be obtained by slow diffusion of Et_2O into a MeCN solution of the crude product; the molecular structure of the cation $[\text{Fe}_3(\text{HL})_2\text{L}_2]^{4+}$, determined crystallographically at 133 K, is shown in Figure 1. It

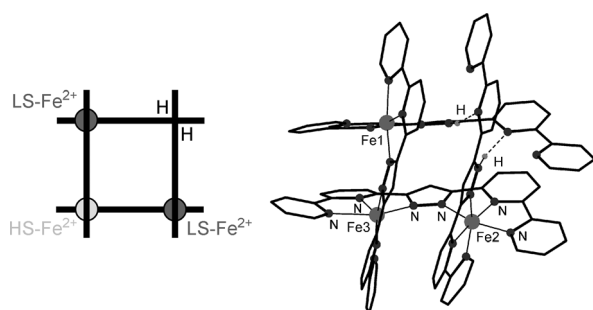


Figure 1. Representation (left) and molecular structure of the defect grid **1** at 133 K determined by X-ray diffraction (right). Counterions and solvent molecules are omitted for clarity.

confirms the gridlike arrangement of four mutually perpendicular ligand strands, but with only three of the four resulting $\{\text{N}_6\}$ binding sites occupied by metal ions. Two interligand $\text{N}^{\text{pz}}\text{--H}\cdots\text{N}^{\text{py}}$ hydrogen bonds are found at the fourth and metal-devoid vertex. The average bond lengths $d(\text{Fe--N})$ for the three crystallographically distinct Fe^{II} ions are 1.96 (Fe1–N), 1.96 (Fe2–N), and 2.18 Å (Fe3–N). Distortion of the $\{\text{FeN}_6\}$ coordination polyhedra away from an ideal octahedron can best be described by the continuous symmetry measure (CSM);^[19] the $S(O_h)$ parameter is 2.18 for Fe1, 2.19 for Fe2, and 6.08 for Fe3. Both $d(\text{Fe--N})$ and $S(O_h)$ clearly reveal a [LS–HS–LS] configuration with the HS– Fe^{II} located at the central metal ion position Fe3 within the defect-grid structure.^[20] At least two acetonitrile molecules per **1** cocrystallize in the lattice; as will be shown below, this is relevant for the magnetic properties.

Several features of **1** caught our attention and stimulated detailed studies of the magnetic properties of this remarkable compound: 1) The mixed-spin situation in an unprecedented and elastically coupled trimetallic arrangement suggested the potential of cooperative SCO; 2) the "structurally soft" character of the H-bonding at the fourth vertex, which is elastically coupled to the metal ions via the pyrazolate

bridges, suggested that the SCO might be affected by external stimuli; and 3) the dangling pyridyl groups next to the metal-devoid vertex, with their N atoms amenable to H-bonding, suggested that guest molecules serving as H-bond donors might be readily bound.

Magnetic susceptibility measurements^[21] for intact **1**·MeCN, collected on freshly crystallized material that was sealed with a small amount of mother liquor in an NMR tube to prevent solvent loss, showed a nearly constant $\chi_M T$ value of around $3.1 \text{ cm}^3 \text{ K mol}^{-1}$. In agreement with the crystallographic data, this indicates a [1HS–2LS] configuration that is stable over the full temperature range between 2 and 380 K. The desolvated solid sample **1** can be obtained by heating **1**·MeCN in the lab prior to use, or in situ inside the SQUID magnetometer by using a sample holder that is not gastight (which is the common situation; note the low pressure of ca. 2.5 mbar He in common MPMS magnetometers during data collection). The desolvated sample **1** shows a complete and sharp SCO of one Fe^{II} ion characterized by a rise of $\chi_M T$ from 3.11 to $6.34 \text{ cm}^3 \text{ K mol}^{-1}$ at $T^\uparrow = 355 \text{ K}$. Upon cooling, $\chi_M T$ goes back to $3.12 \text{ cm}^3 \text{ K mol}^{-1}$ at $T^\downarrow = 329 \text{ K}$, which reflects a complete and reversible thermally induced SCO between the [1HS–2LS] to the [2HS–1LS] states with a 26 K broad hysteresis above room temperature (Figure 2).

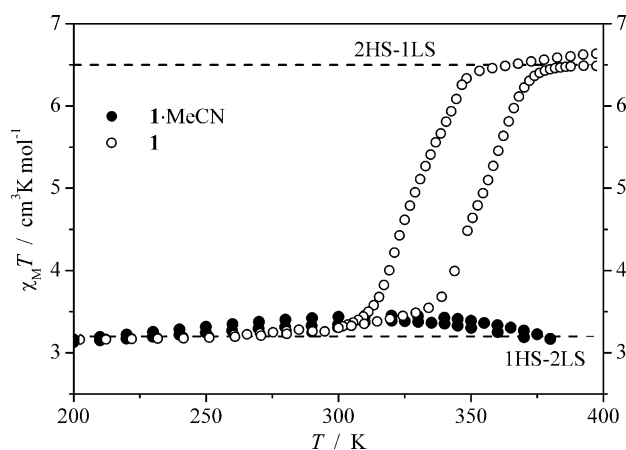


Figure 2. Magnetic data of **1**·MeCN with mother liquor in a sealed sample holder (filled circles) and desolvated **1** (open circles) between 200 and 380 K. Dashed lines show the expected $\chi_M T$ values for the [1HS–2LS] and [2HS–1LS] situations as a guide.

Detailed Mössbauer studies in the temperature range from 6 to 400 K were performed on desolvated single crystalline material of **1** (Figure S4 in the Supporting Information). In order to collect Mössbauer spectra in the high temperature regime (above 300 K), ^{57}Fe enriched samples had to be used. In heating mode, in between 7 and 340 K two quadrupole doublets assigned to LS– Fe^{II} (LS; $\delta = 0.35 \text{ mm s}^{-1}$; $\Delta E_Q = 0.91 \text{ mm s}^{-1}$ at 80 K, blue subspectrum in the left part of Figure 3) and HS– Fe^{II} (HS(A); $\delta = 1.03 \text{ mm s}^{-1}$; $\Delta E_Q = 2.93 \text{ mm s}^{-1}$ at 80 K, red subspectrum) are observed, with a LS/HS(A) ratio of 2:1 in accordance with the crystallographic and magnetic data. At 400 K, an additional doublet appears ($\delta = 0.86 \text{ mm s}^{-1}$; $\Delta E_Q = 1.31 \text{ mm s}^{-1}$ at 400 K, green

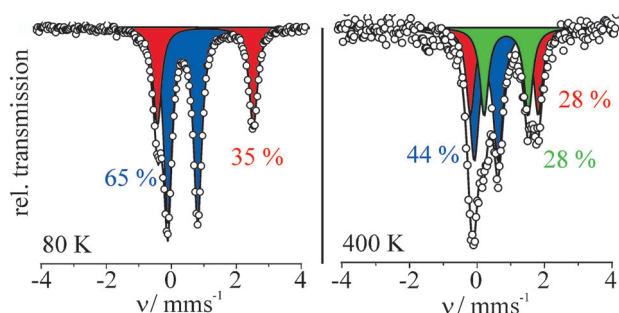


Figure 3. Mössbauer spectra measured at 80 K (left) and beyond the SCO transition at 400 K (right); blue subpeaks: LS-Fe^{II}; red and green subpeaks: HS-Fe^{II}.

subspectrum in Figure 3) for a new HS-Fe^{II} species HS(B). The LS/HS(A)/HS(B) ratio is 44:28:28. The deviation from the expected 1:1:1 ratio can be readily explained by higher Lamb-Mössbauer factors for LS-Fe^{II} compared to HS-Fe^{II} at such high temperatures.

In principle, the magnetic properties observed for **1** might also be explained by an alternative scenario in which 50 % of the bulk material switches to the [3HS] state while 50 % remains in the [1HS-2LS] state. However, for this scenario one should expect to see more than two distinct HS species in the Mössbauer spectra, namely the central HS-Fe^{II} in [1HS-2LS], the central HS-Fe^{II} in [3HS] as well as the outer HS-Fe^{II} in [3HS].^[22] Since only two HS subspectra are observed experimentally (Figure 3, right), we conclude that the SCO process is a complete (i.e., 100 %) [1HS-2LS] to [2HS-1LS] transition. Mössbauer spectra for frozen MeCN solutions of **1** at 80 and 200 K are similar to the spectra for solid material at those temperatures, with two quadrupole doublets assigned to LS and HS(A) and a LS/HS(A) ratio of 2:1 (Figure S5 in the Supporting Information). This result indicates that the [1HS-2LS] configuration is not a result of solid state effects, but represents the intrinsic ground state of **1** in that temperature range.

Interestingly, when a sample of **1** was repeatedly shuttled back and forth through the hysteresis range (200–400 K)

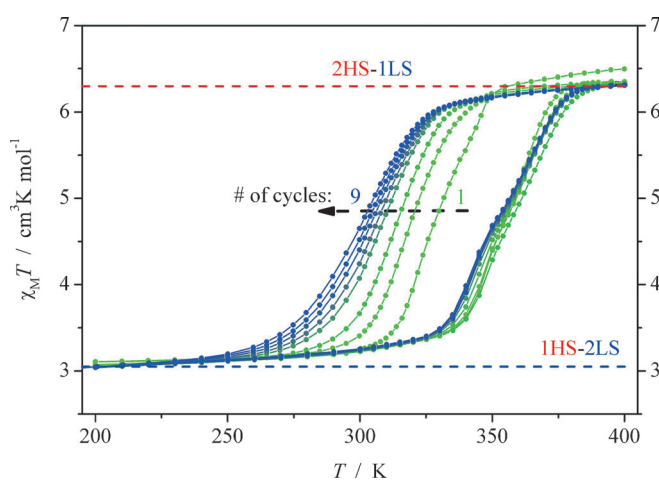


Figure 4. Widening of the hysteresis loop of **1** during nine cycles of repeated heating and cooling in the range 200–400 K.

within the SQUID magnetometer, the broadness of the SCO hysteresis increases with every additional cycle to reach $\Delta T = 49$ K after nine cycles (Figure 4). It is noteworthy that only the transition temperature in cooling mode is shifted, while in heating mode T_{\uparrow} remains roughly constant at 355 K; the largest shift of T_{\downarrow} (by 9 K) is observed between the first and second cycle, with a further shift of around 2 K per subsequent cycle. Concomitantly the SCO becomes slightly more gradual (Figure 4). Since the width of the hysteresis appeared to still increase after the ninth cycle, the sample was heated to 400 K with subsequent cooling to 200 K for 15 more times under vacuum outside the SQUID magnetometer, in an attempt to reach the final state with the broadest hysteresis. Afterwards the sample was reinserted into the SQUID and two more cycles were measured which surprisingly showed a further gradual widening of the hysteresis by 2 and 3 K, respectively, resulting in $\Delta T = 54$ K (Figure S7 in the Supporting Information). Since it was observed that the large single crystals of **1**·MeCN were disaggregated after the measurement, a possible correlation between crystal size and broadness of the hysteresis loop was investigated. To this end, a batch of freshly crystallized material was divided into two parts: the first half was measured without any further preparation, while the second half was carefully pestled. The ground sample indeed showed a much broader (but also more gradual) hysteresis loop than the untreated pristine sample (hysteresis width 33 K versus 24 K; Figure S8), which suggests that the hysteresis becomes broader with decreasing crystal size, and that crystals gradually disaggregate upon iterated thermal cycling through the hysteresis range. Of course, this change can only be reversed by renewed crystallization of the material. It should be noted that besides the hysteretic SCO at around 300–350 K, an additional incomplete and gradual SCO of about 30 % emerges at 110 K after the sample has undergone several heating cycles (Figures S9 and S10); this additional feature could not be explained yet.

In view of the drastically different magnetic properties of pristine **1**·MeCN and desolvated **1**, and since changes in SCO properties induced by host–guest interactions attract considerable current interest, the effect of different solvents on the SCO transition of **1** was investigated. To this end, around 20 mg of compound **1**·MeCN^[21] per experiment were placed in an NMR tube, heated under vacuum for 30 min to generate desolvated **1**, and then exposed to the solvent vapor of choice (with the intrinsic vapor pressure of that solvent at room temperature) to give **1**-solv; finally the tube was sealed and SQUID data were collected. All used solvents (solv = H₂O, MeOH, EtOH, MeCN, acetone, and benzene) were found to inhibit the SCO transition, albeit to different extent. Molecules that are prone to form strong H-bonds were found to silence the SCO transition almost completely (remaining 4 % SCO for **1**·MeOH, 7 % for **1**·H₂O, 8 % for **1**·acetone, 17 % for **1**·EtOH at 400 K); for molecules with lower propensity of forming H-bonds such as benzene and MeCN, **1**-solv shows a gradual and incomplete SCO up to 33 % and 38 % at 400 K, respectively (Figure 5 and Figure S11). Opening the tube to allow for solvent release and remeasuring SQUID data shows that the process is reversible, and that the original hysteresis is fully recovered (Figure S12).

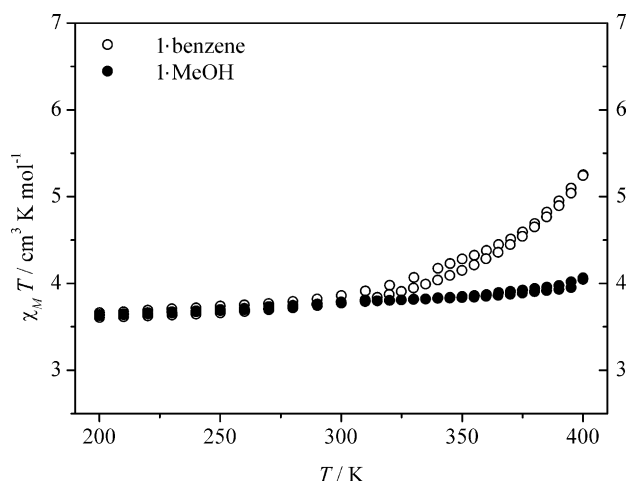


Figure 5. Magnetic data for samples of **1** that have been exposed to benzene (open circles) or MeOH (black circles) between 200 and 380 K.

Interestingly, the SCO is rapidly silenced by exposing, for just 2 min, solid desolvated material **1** in an open vessel to air of ambient humidity (the vessel was then sealed for data collection to avoid water loss upon heating to 400 K in the SQUID). Thermogravimetric analysis (TGA) of solid **1** after exposure to air is in accordance with the presence of around 1.3 equivalents of water, which are smoothly lost in the temperature range 330–400 K, thus suggesting the approximate composition **1**·H₂O after water take-up (Figure S13 in the Supporting Information). Compound **1**·H₂O shows sharp IR bands at 3555 cm⁻¹ and 3622 cm⁻¹, which are absent in spectra of **1**·MeCN and desolvated **1** (Figures S14 and S15). Attenuated total reflection (ATR) spectra collected for **1**·H₂O within a glovebox further show that water uptake is readily reversible: if **1**·H₂O is kept in an atmosphere of dry argon the spectrum of desolvated **1** is restored after 20 min (Figure S15). As a final experiment for unraveling the effect of water on the SCO properties, an air-exposed sample

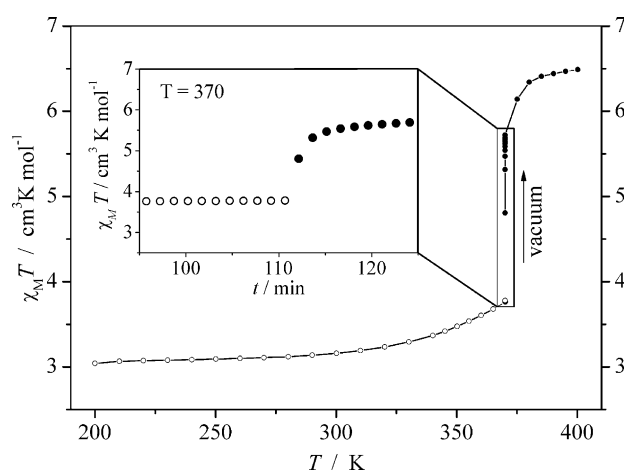


Figure 6. In situ desolvation of **1**·H₂O to give **1** inside of the SQUID magnetometer. Open circles show the measurements at ambient pressure of He, solid circles are measurements under vacuum (ca. 2.5 mbar). Inset: isotherm $\chi_M T$ vs. time at 370 K.

(**1**·H₂O) was inserted into the SQUID, but contained in a sample holder that was not airtight, and under ambient pressure of He. The sample was then heated up to 370 K, whereupon $\chi_M T$ increased just slightly by about 22 % (Figure 6). Then the temperature was held constant at 370 K for 15 min, and while doing so no further change of $\chi_M T$ was observed. Finally the SQUID sample chamber was set under vacuum (ca. 2.5 mbar) while keeping the temperature constant at 370 K, and SCO rapidly took place within 15 min, reflecting how the loss of water induces SCO in **1** (Figure 6, inset). Because of the short response time of **1** upon exposure to air, the smooth reversibility of water uptake, and since the humidity of air under ambient conditions is sufficient to completely silence the SCO, **1** appears to feature favorable characteristics for magnetic sensing of solvent vapor.

In conclusion, a novel type of oligonuclear SCO system is reported, namely the defect-grid Fe^{II}₃ complex **1** that introduces a new motif to the field of grid-type coordination chemistry. **1** features a unique combination of 1) a matrix-like arrangement of switchable sites, which are strongly elastically coupled via bridging pyrazolate ligands, 2) a built-in “structurally soft” metal-devoid vertex, and 3) dangling groups amenable to H-bonding next to the “structurally soft” vertex. Overall this gives rise to a cooperative SCO transition of desolvated **1**; SCO occurs slightly above room temperature and with large thermal hysteresis, and it is readily silenced by the presence of various small molecules. The high sensitivity towards those guest molecules, the short response time upon exposure, and the smooth reversibility of guest binding are favorable characteristics for future sensing applications of such defect grids. An additional interesting observation is the continuous widening of the SCO hysteresis upon repeated thermal cycling through the hysteresis range, which calls for further investigations.

Experimental Section

Synthesis of [Fe₃(HL)₂L₂](BF₄)₄ (1**):** Under an inert atmosphere of dry dinitrogen, NaOtBu (53 mg, 550 μmol, 0.50 equiv) was added to a solution of HL (400 mg, 1.06 mmol, 1.0 equiv) in MeCN (50 mL). This solution was added to a solution of Fe(BF₄)₂·6H₂O (267 mg, 790 μmol, 0.75 equiv) in MeCN (20 mL). The reaction mixture was stirred overnight and then filtered under ambient conditions. The crystalline material **1**·MeCN was obtained by layering the MeCN solution containing the crude product with Et₂O (yield: 63 % of crystalline material). ESI-MS (MeCN solution): 417.9 (100) [Fe₃(HL)₂L₂]⁴⁺, 404.2 (45), 556.7 (30) [Fe₃(HL)L₃]³⁺, 433.1 (25), 807.2 (20) [Fe(HL)L]⁺. UV/vis (MeCN): λ_{max} /nm (ϵ /(L mol⁻¹ cm⁻¹)) = 233 (121000), 263 (88700), 310 (73100), 501 (10100), 627 (2920). Anal. Calcd (%) for **1**·(H₂O)_{1.3}: C, 54.10; H, 3.19; N, 16.46. Found: C, 53.32; H, 3.18; N, 16.44. The water content is derived from the TGA data (see Figure S13).

Received: March 6, 2014

Revised: April 30, 2014

Published online: May 22, 2014

Keywords: cooperative effects · iron · magnetic properties · oligonuclear complexes · spin crossover

- [1] P. Gütllich, H. A. Goodwin, *Top. Curr. Chem.* **2004**, *233*, 1–47.
- [2] K. S. Murray, C. J. Kepert, *Top. Curr. Chem.* **2004**, *233*, 195–228.
- [3] J. A. Real, A. B. Gaspara, M. C. Munoz, *Dalton Trans.* **2005**, 2062–2079.
- [4] Some mononuclear Fe^{II} SCO complexes with a wide thermal hysteresis have been reported: a) M. Sorai, J. Ensling, K. M. Hasselbach, P. Gütllich, *Chem. Phys.* **1977**, *20*, 197–208; b) B. Weber, W. Bauer, J. Obel, *Angew. Chem.* **2008**, *120*, 10252–10255; *Angew. Chem. Int. Ed.* **2008**, *47*, 10098–10101; c) M. B. Bushuev, V. A. Daletsky, D. P. Pishchur, Y. V. Gatilov, I. V. Korolkov, E. B. Nikolaenkova, V. P. Krivopalov, *Dalton Trans.* **2014**, *43*, 3906–3910.
- [5] a) J. Olguín, S. Brooker in *Spin-Crossover Materials: Properties and Applications* (Ed.: M. A. Halcrow), Wiley, Chichester, **2013**, p. 77; b) V. Ksenofontov, A. B. Gaspar, V. Niel, S. Reiman, J. A. Real, P. Gütllich, *Chem. Eur. J.* **2004**, *10*, 1291–1298; c) K. S. Min, K. Swierczek, A. G. DiPasquale, A. L. Rheingold, W. M. Reiff, A. M. Arif, J. S. Miller, *Chem. Commun.* **2008**, 317–319; d) B. Weber, E. S. Kaps, J. Obel, K. Achterhold, F. G. Parak, *Inorg. Chem.* **2008**, *47*, 10779–10787; e) Y. Sunatsuki, R. Kawamoto, K. Fujita, H. Maruyama, T. Suzuki, H. Ishida, M. Kojima, S. Iijima, N. Matsumoto, *Inorg. Chem.* **2009**, *48*, 8784–8795; f) C. J. Schneider, B. Moubaraki, J. D. Cashion, D. R. Turner, B. A. Leita, S. R. Batten, K. S. Murray, *Dalton Trans.* **2011**, *40*, 6939–6951; g) R. Kulmaczewski, J. Olguín, J. A. Kitchen, H. L. C. Feltham, G. N. L. Jameson, J. L. Tallon, S. Brooker, *J. Am. Chem. Soc.* **2014**, *136*, 878–881.
- [6] S. Kanegawa, S. Kang, O. Sato, *Eur. J. Inorg. Chem.* **2013**, 725–729.
- [7] a) D. Savard, C. Cook, G. D. Enright, I. Korobkov, T. J. Burchell, M. Murugesu, *CrystEngComm* **2011**, *13*, 5190–5197; b) Y. Garcia, P. Guionneau, G. Bravic, D. Chasseau, J. A. K. Howard, O. Kahn, V. Ksenofontov, S. Reiman, P. Gütllich, *Eur. J. Inorg. Chem.* **2000**, 1531–1538; c) J. J. A. Kolnaar, G. van Dijk, H. Kooijman, A. L. Spek, V. G. Ksenofontov, P. Gütllich, J. G. Haasnoot, J. Reedijk, *Inorg. Chem.* **1997**, *36*, 2433–2440; d) G. Psomas, N. Bréfuel, F. Dahan, J.-P. Tuchagues, *Inorg. Chem.* **2004**, *43*, 4590–4594; e) G. Vos, R. A. G. de Graaff, J. G. Haasnoot, A. M. van der Kraan, P. de Vaal, J. Reedijk, *Inorg. Chem.* **1984**, *23*, 2905–2910; f) G. Vos, R. A. le Fèvre, R. A. G. de Graaff, J. G. Haasnoot, J. Reedijk, *J. Am. Chem. Soc.* **1983**, *105*, 1682–1683; g) M. Thomann, O. Kahn, J. Guilhem, F. Varret, *Inorg. Chem.* **1994**, *33*, 6029–6037.
- [8] a) E. Breuning, M. Ruben, J.-M. Lehn, F. Renz, Y. Garcia, V. Ksenofontov, P. Gütllich, E. Wegelius, K. Rissanen, *Angew. Chem.* **2000**, *112*, 2563–2566; *Angew. Chem. Int. Ed.* **2000**, *39*, 2504–2507; b) M. Nihei, M. Ui, M. Yokota, L. Han, A. Maeda, H. Kishida, H. Okamoto, H. Oshio, *Angew. Chem.* **2005**, *117*, 6642–6645; *Angew. Chem. Int. Ed.* **2005**, *44*, 6484–6487; c) D.-Y. Wu, O. Sato, Y. Einaga, C.-Y. Duan, *Angew. Chem.* **2009**, *121*, 1503–1506; *Angew. Chem. Int. Ed.* **2009**, *48*, 1475–1478; d) I. Boldog, F. J. Muñoz-Lara, A. B. Gaspar, M. C. Muñoz, M. Seredyuk, J. A. Real, *Inorg. Chem.* **2009**, *48*, 3710–3719; e) R.-J. Wei, Q. Huo, J. Tao, R.-B. Huang, L.-S. Zheng, *Angew. Chem.* **2011**, *123*, 9102–9105; *Angew. Chem. Int. Ed.* **2011**, *50*, 8940–8943; f) A. Mondal, Y. Li, P. Herson, M. Seuleiman, M.-L. Boillot, E. Rivière, M. Julve, L. Rechignat, A. Bousseksou, R. Lescouëzec, *Chem. Commun.* **2012**, *48*, 5653–5655; g) Y.-T. Wang, S.-T. Li, S.-Q. Wu, A.-L. Cui, D.-Z. Shen, H.-Z. Kou, *J. Am. Chem. Soc.* **2013**, *135*, 5942–5945.
- [9] B. Schneider, S. Demeshko, S. Dechert, F. Meyer, *Angew. Chem.* **2010**, *122*, 9461–9464; *Angew. Chem. Int. Ed.* **2010**, *49*, 9274–9277.
- [10] B. Schneider, S. Demeshko, S. Neudeck, S. Dechert, F. Meyer, *Inorg. Chem.* **2013**, *52*, 13230–13237.
- [11] R.-J. Wei, J. Tao, R.-B. Huang, L.-S. Zheng, *Eur. J. Inorg. Chem.* **2013**, 916–926.
- [12] M. Ruben, J. Rojo, F. J. Romero-Salguero, L. H. Uppadine, J.-M. Lehn, *Angew. Chem.* **2004**, *116*, 3728–3747; *Angew. Chem. Int. Ed.* **2004**, *43*, 3644–3662.
- [13] G. J. Hardy, *Chem. Soc. Rev.* **2013**, *42*, 7899.
- [14] M. A. Halcrow, *Chem. Soc. Rev.* **2011**, *40*, 4119–4142.
- [15] a) W. Vreugdenhil, J. H. Van Diemen, R. A. G. De Graaff, J. G. Haasnoot, J. Reedijk, A. M. Van Der Kraan, O. Kahn, J. Zarembowitch, *Polyhedron* **1990**, *9*, 2971–2979; b) G. J. Halder, C. J. Kepert, B. Moubaraki, K. S. Murray, J. D. Cashion, *Science* **2002**, *298*, 1762–1765.
- [16] a) R.-J. Wei, J. Tao, R.-B. Huang, L.-S. Zheng, *Inorg. Chem.* **2011**, *50*, 8553–8564; b) J. S. Costa, S. Rodríguez-Jiménez, G. A. Craig, B. Barth, C. M. Beavers, S. J. Teat, G. Aromí, *J. Am. Chem. Soc.* **2014**, *136*, 3869–3874.
- [17] J. I. van der Vlugt, S. Demeshko, S. Dechert, F. Meyer, *Inorg. Chem.* **2008**, *47*, 1576–1585.
- [18] B. Schneider, S. Demeshko, S. Dechert, F. Meyer, *Inorg. Chem.* **2012**, *51*, 4912–4914.
- [19] a) S. Alvarez, D. Avnir, M. Llunell, M. Pinsky, *New J. Chem.* **2002**, *26*, 996–1009; b) H. Zabrodsky, S. Peleg, D. Avnir, *J. Am. Chem. Soc.* **1992**, *114*, 7843–7851; c) H. Zabrodsky, S. Peleg, D. Avnir, *J. Am. Chem. Soc.* **1993**, *115*, 8278–8289.
- [20] O. Kahn, *Molecular Magnetism*, VCH, Weinheim, **1993**.
- [21] For all magnetic studies, single-crystalline material obtained by Et₂O diffusion was used, because the crude powder or polycrystalline material only showed gradual and incomplete SCO (Figure S6).
- [22] C. M. Grunert, S. Reiman, H. Spiering, J. A. Kitchen, S. Brooker, P. Gütllich, *Angew. Chem.* **2008**, *120*, 3039–3041; *Angew. Chem. Int. Ed.* **2008**, *47*, 2997–2999.